



COVER SHEET

This is the author version of article published as:

Hu, Y.Q. and Yan, Cheng and Zhang, H.F. and Ye, L. and Hu, Z.Q.
(2004) Preparation and hydrogenation characteristics of Mg–30 wt.%
Ti37.5V25Cr37.5 composite. *Journal of Alloys and Compounds* 375(1-
2):pp. 265-269.

Copyright 2004 Elsevier

Accessed from <http://eprints.qut.edu.au>

Preparation and Hydrogenation Characteristics of Mg-30mass% Ti_{37.5}V₂₅Cr_{37.5} Composite

Y.Q. Hu^{a,b*}, C. Yan^b, H.F. Zhang^a, L. Ye^b, Z.Q. Hu^a

^a*Shenyang National Laboratory for Materials Science, Institute of Metal Research, Chinese Academy of Sciences, Shenyang, 110016, China*

^b*Centre for Advanced Materials Technology, School of Aerospace, Mechanical and Mechatronic Engineering, J07, The University of Sydney, NSW 2006, Australia*

Abstract: A Mg-30mass% Ti_{37.5}V₂₅Cr_{37.5} hydrogen storage composite was successfully synthesized by reactive mechanical milling of a mixture of magnesium and Ti_{37.5}V₂₅Cr_{37.5} powder in a hydrogen atmosphere. The structural evolution during milling and after hydrogen absorption/desorption cycling was analyzed using XRD. The absorption/desorption rates and storage capacity at different temperatures were evaluated. By analyzing the variation of Avrami exponent, the hydrogenation mechanisms during milling process were also estimated. A large hydrogen storage capacity and excellent absorption/desorption kinetics were achieved in this composite.

KEYWORDS: Mg-based alloys, hydrogen storage materials, reaction ball milling, catalyst, absorption kinetics.

1. Introduction

-
- Corresponding author.
 - E-mail address: huyeqi@imr.ac.cn

Magnesium and Mg-based hydrogen storage materials have attracted increasing attention due to their high hydrogen storage capacity and low cost [1]. Unfortunately, high working temperature, slow reaction kinetics and hard activation processes limit the practical application of Mg-based hydride system. Fujii et al. [2] designed a multi-layer Pd/Mg thin film that could absorb hydrogen up to about 5 mass% at 373 K under a hydrogen pressure of 0.1MPa and desorb all hydrogen at 360 K in vacuum. Zhu et al. [3] also confirmed that Mg or $Mm_{17}Mg_2$ could absorb hydrogen even at room temperature. Many investigations have been carried out to understand the possibility of developing Mg-based composites by adding second phases into Mg matrix, such as Mg-Mg₂Ni_{0.75}Fe_{0.25} [4], Mg-LaNi₅ [5], Mg-FeTi [6] and Mg-TiMn_{1.5} [7]. In these studies, apparent advances in hydrogen absorption capacity and kinetics have been achieved due to the existence of second phase additives although the hydrogen absorption mechanisms might be very different.

Recently, alloys with bcc (body-centered-cubic) structures have been studied widely due to their intrinsic capacity for hydrogen storage [8-11]. It has been reported that some Ti-V-Cr and Ti-V-Mn alloys exhibit large hydrogen capacities of over 2 mass% and excellent kinetics at relatively lower working temperature [12-16]. This implies that alloys with a bcc structure may be used as second phase additives to gain both high hydrogen storage capacity and excellent reaction kinetics in Mg-based composites.

Traditionally, reactive ball milling (RBM) method has been extensively used to prepare metallic materials with metastable phases. This method has also been

successfully introduced to prepare hydrogen storage materials [17, 18]. It combines the courses of sample preparation, activation and hydrogenation into one step. Mg particles can be easily transformed into brittle hydrides with nano-sized grains during RBM. Furthermore, the alloy powder can be in-situ activated during RBM.

It has been demonstrated that a bcc structured $\text{Ti}_{37.5}\text{V}_{25}\text{Cr}_{37.5}$ alloy possesses excellent hydriding/dehydriding properties at moderate temperature [19]. In this work, the $\text{Ti}_{37.5}\text{V}_{25}\text{Cr}_{37.5}$ alloy was produced by casting. The as-cast ingots were crushed into powder. Both $\text{Ti}_{37.5}\text{V}_{25}\text{Cr}_{37.5}$ and Mg powders were mixed and mechanically milled under hydrogen atmosphere. Finally, a nano-grained composite with fine $\text{Ti}_{37.5}\text{V}_{25}\text{Cr}_{37.5}$ particles uniformly dispersed on the surface of Mg particles was successfully produced.

2. Experimental procedure

2.1 Materials

$\text{Ti}_{37.5}\text{V}_{25}\text{Cr}_{37.5}$ alloy was prepared by arc melting with electromagnetic stirring (EMS) in an argon atmosphere using materials with high purity (>99.9%). The ingots were turned upside down and melted four times to ensure homogeneity. The as-cast ingots were crushed into fine powder passing through a 0.5mm screen. Then, powders of the as-cast alloy (30 mass %) and Mg (100 mesh) were put into a stainless steel vial with ball to powder ratio of 20:1. The vial was sealed by an O-ring and connected to a gas reservoir with an initial pressure of 1 MPa. The total volume of the system was 260 cm^3 , and the total milling time was 5 h using a SPEX8000 miller. The variation of

hydrogen pressure due to the absorption of hydrogen by the powder was monitored continuously. For comparison, the as-cast $\text{Ti}_{37.5}\text{V}_{25}\text{Cr}_{37.5}$ alloy was separately milled under the same condition.

2.2 Sample characterization

At selected time, small amounts of powder were taken out of the vial to characterize the sample. The structural evolution during milling was examined using a Rigaku X-ray diffractometer equipped with graphite monochromator with Cu α radiation. The microstructures were observed using SEM (PHILIPS XL 30CP) equipped with an energy dispersive X-ray analysis system and TEM (PHILIPS EM420). Hydriding/dehydriding properties of the composite were measured at different temperatures using a conventional volumetric method.

3. Results and discussion

3.1 Structural evolution during reactive ball milling

The XRD spectra as a function of milling time for the $\text{Mg-Ti}_{37.5}\text{V}_{25}\text{Cr}_{37.5}$ under hydrogen atmosphere are shown in Fig. 1. Tetragonal $\beta\text{-MgH}_2$ and hydrides of $\text{Ti}_{37.5}\text{V}_{25}\text{Cr}_{37.5}$ are generated after 1 h milling. The relative intensity of Mg decreases and the peaks broaden drastically after 2 h milling. The reduction of relative intensity of Mg is attributed to hydriding and reduction of grain size. After 5 h milling, XRD patterns of Mg almost disappear and nano-sized $\beta\text{-MgH}_2$ and hydrides of $\text{Ti}_{37.5}\text{V}_{25}\text{Cr}_{37.5}$ become the principal components of the composite. The patterns of Fe

can be observed after 5 h milling, indicating that iron contamination may occur after long time milling. The crystal size of β -MgH₂ milled for 5 h has been estimated as about 10 nm using the Scherer's equation.

The XRD patterns of Ti_{37.5}V₂₅Cr_{37.5} alloy milled in a hydrogen atmosphere are shown in Fig. 2. The patterns of hydrides of Ti_{37.5}V₂₅Cr_{37.5} exist in the initial stage of milling, indicating the Ti_{37.5}V₂₅Cr_{37.5} alloy powder to be easily hydrided by mechanical energy. The relative intensity for the Ti_{37.5}V₂₅Cr_{37.5} alloy and its hydrides remains stable after 5 h milling.

3.2 Absorption kinetic during reactive ball milling

During RBM, the hydrogen pressure was measured by a pressure transducer; the weight of hydrogen absorbed, as a function of milling time, can be evaluated as:

$$W_H\% = (100m_H\Delta PV)/(MRT)\%, \quad (1)$$

where m_H is the atomic mass of hydrogen, ΔP is the change of pressure, V is the volume of the system, M is the initial powder mass, R is the gas constant and T is the temperature.

The time dependence of the hydrogen absorption during the milling is shown in Fig. 3. In the initial 10 min, about 1.05 wt % of hydrogen is absorbed quickly; then, the hydrogen absorption is slowed down in the following 1 h. The hydrogen content increases more rapidly during the period of 1 h to 3 h, and a saturated value of up to 6.39 wt % is finally achieved.

Hydrogen absorption of the $\text{Ti}_{37.5}\text{V}_{25}\text{Cr}_{37.5}$ alloy during RBM was also investigated. About 3.52 wt % hydrogen was absorbed during the first 10 min milling, and no appreciated hydrogen was absorbed after that. Therefore, for the mixture of Mg and $\text{Ti}_{37.5}\text{V}_{25}\text{Cr}_{37.5}$, hydrogen was mainly absorbed by the $\text{Ti}_{37.5}\text{V}_{25}\text{Cr}_{37.5}$ alloy in the initial 10 min and the later absorption was attributed to Mg. In Fig. 2, it can be also seen that the XRD patterns of hydrides of $\text{Ti}_{37.5}\text{V}_{25}\text{Cr}_{37.5}$ exist at the beginning of the milling and keep stable in the remaining time. Considering the theoretical capacity of hydrogen absorption of Mg, it is clear that Mg particles are transformed into hydrides completely due to the catalysis effect of $\text{Ti}_{37.5}\text{V}_{25}\text{Cr}_{37.5}$ alloy and the high mechanical energy.

According to Johnson-Mehl-Avrami equation [20], Avrami exponent (n) can be estimated in a milling process. In this work, the calculated value of n is in the range of 1.5~2.3 during reaction ball milling [21]. Based on the relationship between Avrami exponent (n) and transformation type proposed by Christian [22], hydrogenation mechanism in this Mg-based composite is mainly a three-dimensional growth mechanism controlled by the diffusion of hydrogen atom during reactive ball milling.

3.3 Structural evolution and microstructure characteristics

The structural evolution of Mg- $\text{Ti}_{37.5}\text{V}_{25}\text{Cr}_{37.5}$ during hydrogen absorption/desorption process was also investigated using XRD analysis, as shown in Fig. 4. The patterns b and c are for the samples hydrogenated and dehydrogenated at 573 K after twenty cycles, respectively. It can be seen that most magnesium has been hydrogenated at

573 K so that the intensity of Mg peaks in pattern b is remarkably reduced. In Fig. 4 (b), the patterns of hydrides of $\text{Ti}_{37.5}\text{V}_{25}\text{Cr}_{37.5}$ still exist at room temperature for the sample experienced hydrogen absorption at 573 K. This may be due to the large hydrogen absorption capacity of $\text{Mg-Ti}_{37.5}\text{V}_{25}\text{Cr}_{37.5}$ at high temperature and hydrogen absorption of $\text{Ti}_{37.5}\text{V}_{25}\text{Cr}_{37.5}$ when the temperature descends from 573K to room temperature. The patterns of hydrides of $\text{Ti}_{37.5}\text{V}_{25}\text{Cr}_{37.5}$ do not appear for the sample experienced hydrogen desorption at 573 K, shown in Fig. 4(c).

Fig.5 shows a SEM image of the composite particles after 5h milling. EDS analysis indicated that there was a concentration of Ti, V and Cr in the bright phases (white dots). It is reasonable to regard these bright phases as $\text{Ti}_{37.5}\text{V}_{25}\text{Cr}_{37.5}$. These fine $\text{Ti}_{37.5}\text{V}_{25}\text{Cr}_{37.5}$ particles are dispersed uniformly on the surfaces of Mg particles. Such ideal microstructure of the composite can be rationally understood as a result of the continuous cold welding and fraction in the milling course. The microstructure and phase composition of the composite were examined by TEM analysis, shown in Fig.6. The bright field image shows that the grain size of Mg is about 10 nm. This is in agreement with the XRD analysis.

3.4 Hydriding/dehydriding properties

After evacuation at 373 K for about an hour, the composite powder was heated up to 573 K. It was found that the composite was dehydrided very fast at 573K. When the hydrogen (2.5 MPa) was introduced for the first time, the sample was hydrided rapidly. The first absorption hydrogen capacity could reach to 4.6 mass% at 573 K.

After two or three absorption/desorption cycles, the sample was activated completely. Usually, the working temperature for Mg-based hydrogen storage composites is above 573 K, and it needs many hours to complete one hydrogen absorption/desorption cycle. These shortcomings have been overcome to a great extent in this work. Fig. 7 shows the hydrogen absorption kinetics curves for the composite at different temperatures. At 573 K, the highest hydrogen absorption reaches 5.7 mass %, and it needs only three minutes to complete 90 % of the final capacity. It is desirable for Mg-based hydrogen storage materials to work at lower temperature. In Fig. 7, it can be observed that even at a moderate temperature (373 K), the composite still has a relatively high hydrogen storage capacity (3.8 mass % under 2.5 MPa hydrogen pressure). It can absorb up to 80 % of the final capacity in two minutes and completes the whole process in ten minutes. At 343 K, the hydrogen absorption capacity reaches 2.36 mass %. As mentioned above, pure $\text{Ti}_{37.5}\text{V}_{25}\text{Cr}_{37.5}$ alloy can absorb hydrogen up to 3.52 mass %. Therefore, the maximum contribution to hydrogen absorption from 30 mass % $\text{Ti}_{37.5}\text{V}_{25}\text{Cr}_{37.5}$ in this composite is about 1 mass %. The rest of hydrogen must be absorbed by Mg at 343 K. Fig. 8 shows that desorption processes only take about 10 min at 543 K and 573 K, respectively. Therefore, the desorption properties were also improved greatly in this work.

The hydrogenation properties don't degrade in the following cycles. Furthermore, the grain size grew up to 30 nm after three cycles, and then remained stable in the rest cycles. The composite was relatively stable during absorption/desorption hydrogen cycles.

3.5 Hydrogenation mechanism

Based on the analyses above, the main hydrided phase was magnesium in the composite and only small amounts of hydrogen was absorbed by $\text{Ti}_{37.5}\text{V}_{25}\text{Cr}_{37.5}$ at moderate temperatures. The $\text{Ti}_{37.5}\text{V}_{25}\text{Cr}_{37.5}$ alloy mainly contributed to the hydrogen absorption as a catalyst.

Due to the high mechanical energy provided by ball milling, fine $\text{Ti}_{37.5}\text{V}_{25}\text{Cr}_{37.5}$ particles can be dispersed uniformly on the surfaces of Mg particles, thus playing a critical role in accelerating the hydrogenation at the initial stage [23, 24]. During a absorption/desorption cycle, the catalytic effect of the $\text{Ti}_{37.5}\text{V}_{25}\text{Cr}_{37.5}$ alloy can be achieved through degrading the dissociation energy of hydrogen molecules and acting as “paths” for diffusion of hydrogen atoms from surfaces to inside of Mg particles [25]. Additionally, nano-grained Mg or MgH_2 were created during the RBM process. The large amount of grain boundaries can increase the active sites of the composite, thus shortening the diffusion distance of hydrogen atoms.

The catalysis mechanisms of the second phase, especially for V element, are not well understood. Liang et al. thought that the enhanced absorption kinetics was attributed to a spill-over effect involving the formation and decomposition of vanadium hydride, thus acting as a hydrogen pump [26]. But Oelerich et al. confirmed that the hydrogen reaction kinetics enhance significantly under the chosen experimental conditions only for V_2O_5 , VN and VC, while the influence of high-purity V is negligible [27]. Fernandez et al. investigated the hydriding/dehydriding properties of Mg-ZrCr_2

composites [28]. The $ZrCr_2$ has an AB_2 structure which is similar to the $TiCr_2$. In comparison with their results, the composite of $Mg-Ti_{37.5}V_{25}Cr_{37.5}$ in this study has an improved absorption/desorption properties. If the influence of high-purity V is negligible, the enhancement of the hydrogen reaction kinetics in our case is due to the compound existence of V element. This fact implies that there may be some unknown relations between the enhancement of hydrogen reaction kinetics and the valence of vanadium as a compound. Oelerich et al [27, 29] also showed that local electronic structures of a catalyst were of great importance for absorption kinetics in Mg-based hydrogen storage composites. Nevertheless, further effort is required to investigate on the effect of valence distribution in a catalyst on the absorption/desorption kinetics.

4. Conclusions

$Mg-Ti_{37.5}V_{25}Cr_{37.5}$ composite was successfully prepared by reaction mechanical alloying. The composite has a high hydrogen storage capacity and excellent absorption/desorption kinetic properties. It can be in situ activated during the reaction ball milling (RBM). The hydrogen capacity is over 3.8 mass% at 373K, and one absorption/desorption hydrogen cycle can be finished in twenty minutes at 543 K~573 K. The enhanced absorption/desorption kinetics and high hydrogen storage capacity can be attributed to the fine grains and imperfections introduced by the high energy ball milling and the catalytic effect of $Ti_{37.5}V_{25}Cr_{37.5}$.

Acknowledgements

This work was carried out under the financial support of National High Technical Research Development Program of China (No. 2001AA331010) and National Key Basic Research and Development Program of China (No.G2000067201). The authors also acknowledge the support of a Sydney University Sesqui R & D grant.

References

- [1] D. A. Small, G. R. Mackay, R. A. Dunlap. *J. Alloys Comps.*, 284 (1999) 312.
- [2] H. Fujii, S. Orimo. *Physica B*, 328 (2003) 77.
- [3] M. Zhu , Y. Gao , X.Z. Che , Y.Q. Yang , C.Y. Chung. *J. Alloys Comps.*, 330–332 (2002) 708.
- [4] H.T. Yuan, H.B. Yang, Z.X. Zhou, D.Y. Song, Y.S. Zhang. *J. Alloys Comp.* 260 (1997) 256.
- [5] G. liang, S. Boily, J. Huot, A.V. Neste, R.Schulz. *J. Alloys Comp.* 268 (1998) 302.
- [6] P. Mandal, O.N. Srivastava. *J. Alloys Comp.* 205 (1994) 111.
- [7] Y.Q. Hu, H.F. Zhang, A.M. Wang, B.Z. Ding, Z.Q. Hu. *J. Alloys Comp.* 354 (2003) 296.
- [8] L. Schlapbach and A. Züttel. *Nature*, 414-15 (2001) 353.
- [9] Y. Tominaga, S. Nishimura, T. Amemiya, T. Fuda. T. Tamura, T. Kuriwa, A. Kamegawa and M. Okada. *Mater. Trans, JIM*, 40-9 (1999) 871.

- [10] E. Akiba and M. Okada. MRS Bulletin, 9 (2002) 699.
- [11] D.S. Dos Santo, M. Bououdina, D. Fruchart. J. Alloys Compd., 340 (2002) 101.
- [12] C.Y. Seo, J.H. Kim, P.S. Lee, J.Y. Lee. J. Alloys Compd., 348 (2003) 252.
- [13] K. Shirasaki, T. Tamura, T. Kuriwa, T. Goto, A. Kamegawa, H. Takamura, M. Okada. Mater. Trans, JIM, 43-5 (2002) 1115.
- [14] H. Iba and E. Akiba. J. Alloys Compd., 253-254 (1997) 21.
- [15] E. Akiba and H. Enoki. Materia Japan, 37 (1998) 645.
- [16] M. Okada, T. Kuriwa, T. Tamura, H. Takamura and A. Kamegawa. Metals and Materials International 7 (2001) 67.
- [17] J.L. Bobet, B. Chevalier, M.Y. Song, B. Darriet, J. Etourneau. J. Alloys Comp. 336 (2002) 292.
- [18] P. Wang, A.M. Wang, H.F. Zhang, B.Z. Ding, Z.Q. Hu. J. Alloys Comp. 313 (2000) 218.
- [19] T. Yukio, N. Sinya, A. Toshikazu. Mater. Trans. JIM., 9 (1999) 871.
- [20] M. Avrami. J. Chem. Phys. 9 (1941) 177.
- [21] Y.Q. Hu, H.F. Zhang, C. Yan, L. Ye, B.Z. Ding, Z.Q. Hu. J. Mater. Sci. Lett. Revised.
- [22] J. W. Christian. The Theory of Transformation in Metals and Alloys, Pergamon Press. Oxford (1965) p. 489.
- [23] M. Zhu, W.H. Zhu, Y. Gao, X.Z. Che, J.H. Ahn. Mater. Sci. Eng. A 286 (2000) 130.
- [24] A. Zaluska, L. Zaluski, J.O. Strom-Olsen. J. Alloys Comp. 288 (1999) 271.

- [25] P.Wang, A.M.Wang, H.F. Zhang. *J. Mater. Sci. Lett.* 20 (8) (2001) 753.
- [26] G. Liang , J. Huot , S. Boily , A. Van Neste , R. Schulz. *J. Alloys Comp.* 291 (1999) 295.
- [27] W. Oelerich , T. Klassen, R. Bormann. *J. Alloys Comp.* 322 (2001) L5.
- [28] J.F. Fernandez , J. Bodega, C.R. Sanchez. *J. Alloys Comp.* 356-357 (2003) 343.
- [29] G. Barkhordarian, T. Klassen, R. Bormann. *Scripta Materialia* 49 (2003) 213.

Caption

Fig. 1 X-ray diffraction patterns of mechanically milled Mg-Ti_{37.5}V₂₅Cr_{37.5} in a hydrogen atmosphere after (a) 1 h, (b) 2 h, (c) 3 h and (d) 5 h milling.

Fig. 2 X-ray diffraction patterns of (a) arc melted Ti_{37.5}V₂₅Cr_{37.5}, (b) mechanically milled Ti_{37.5}V₂₅Cr_{37.5} in a hydrogen atmosphere for 10 min, and (c) mechanically milled Mg and Ti_{37.5}V₂₅Cr_{37.5} in a hydrogen atmosphere for 5 h.

Fig. 3 Hydrogen absorption as a function of milling time for Mg-Ti_{37.5}V₂₅Cr_{37.5} alloy in a hydrogen atmosphere.

Fig. 4 XRD patterns for Mg- Ti_{37.5}V₂₅Cr_{37.5} composite before and after hydriding/dehydriding cycles, (a) milled in a hydrogen atmosphere for 5 h, (b) hydrogenated at 573 K after twenty cycles, and (c) dehydrogenated at 573 K after twenty cycles.

Fig. 5 Scanning electron micrograph of the Mg- Ti_{37.5}V₂₅Cr_{37.5} composite after 5h milling

Fig. 6 TEM results of the composite Mg- Ti_{37.5}V₂₅Cr_{37.5} particle.

Fig. 7 Hydrogen absorption kinetics for Mg-Ti_{37.5}V₂₅Cr_{37.5}.

Fig. 8 Hydrogen desorption kinetics for Mg-Ti_{37.5}V₂₅Cr_{37.5}.

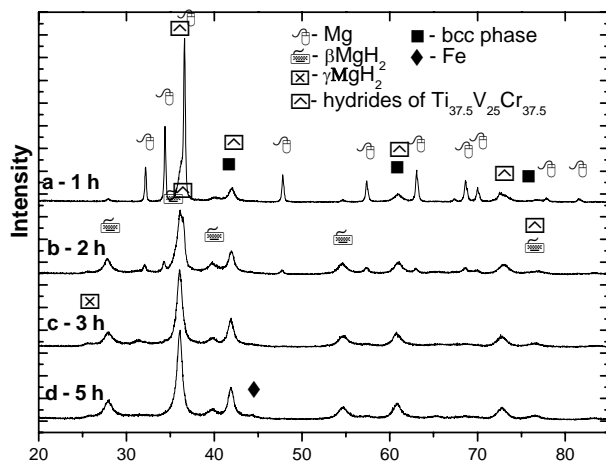
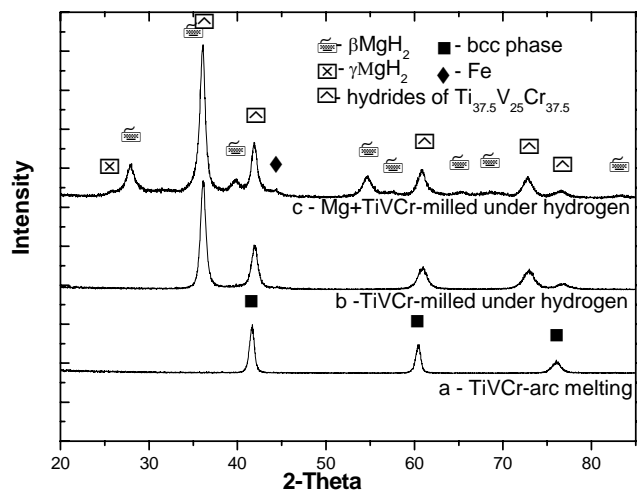


Fig. 1 X-ray diffraction patterns of mechanically milled $\text{Mg-Ti}_{37.5}\text{V}_{25}\text{Cr}_{37.5}$ in a hydrogen atmosphere after (a) 1 h, (b) 2 h, (c) 3 h and (d) 5 h milling.



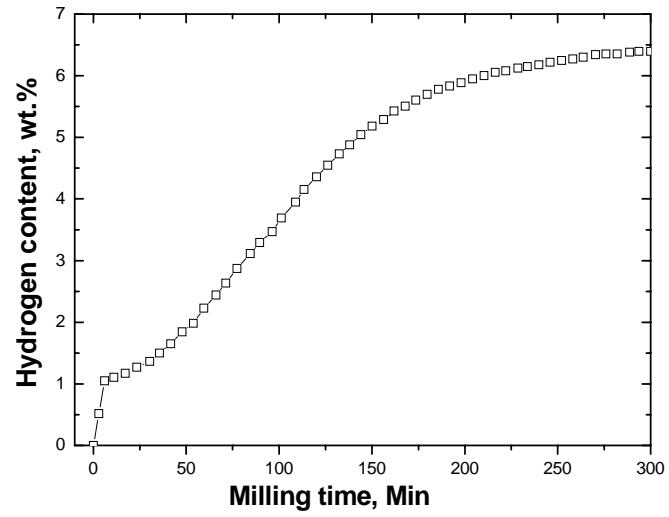


Fig. 3 Hydrogen absorption as a function of milling time for Mg-Ti_{37.5}V₂₅Cr_{37.5} alloy in a hydrogen atmosphere.

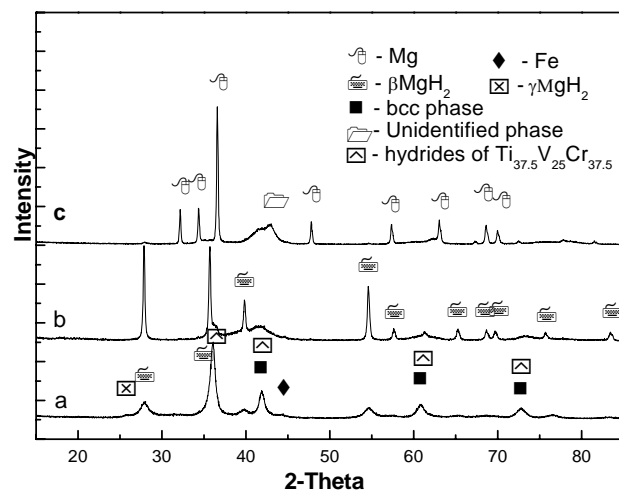


Fig. 4 XRD patterns for Mg- Ti_{37.5}V₂₅Cr_{37.5} composite before and after hydriding/dehydriding cycles, (a) milled in a hydrogen atmosphere for 5 h, (b) hydrogenated at 573 K after twenty cycles, and (c) dehydrogenated at 573 K after twenty cycles.

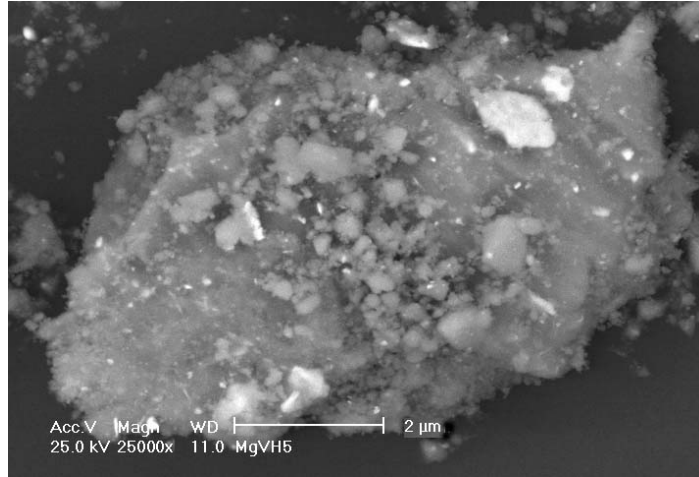


Fig. 5 Scanning electron micrograph of the Mg- Ti_{37.5}V₂₅Cr_{37.5} composite after 5h milling

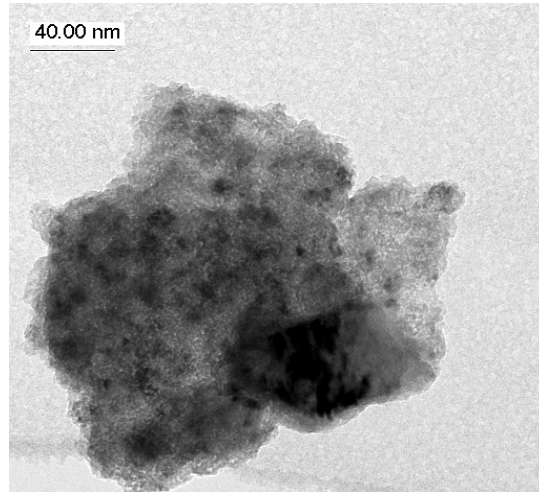


Fig. 6 TEM results of the composite Mg- $\text{Ti}_{37.5}\text{V}_{25}\text{Cr}_{37.5}$ particle.

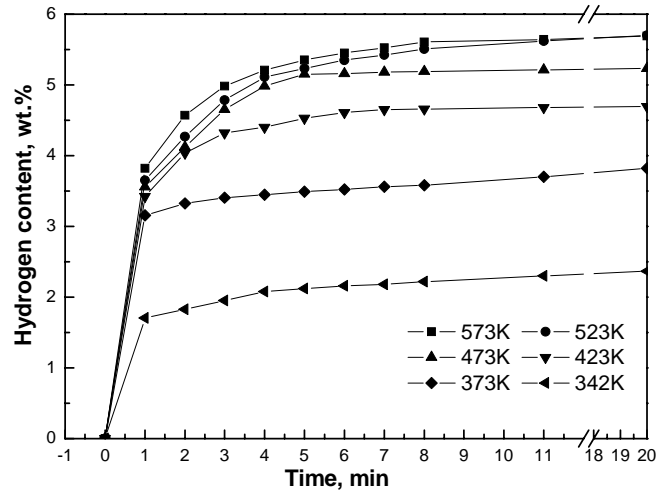


Fig.7 Hydrogen absorption kinetics for Mg-Ti_{37.5}V₂₅Cr_{37.5}.

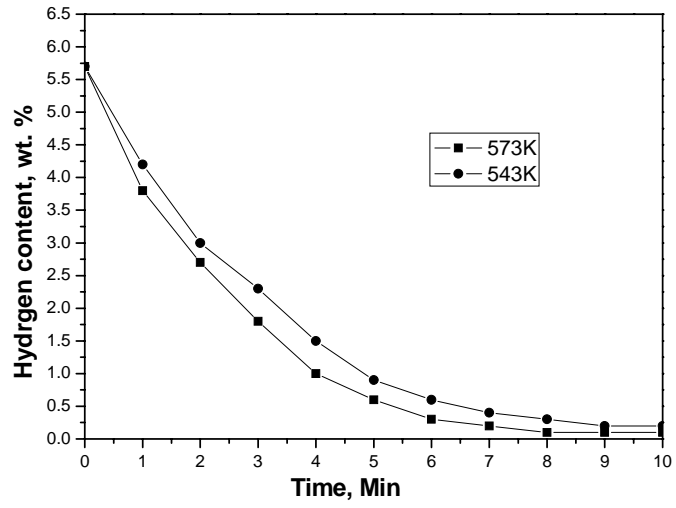


Fig.8 Hydrogen desorption kinetics for Mg-Ti_{37.5}V₂₅Cr_{37.5}.